2302–2310 *Nucleic Acids Research, 1996, Vol. 24, No. 12*

Characterization of several kinds of dimer minizyme: simultaneous cleavage at two sites in HIV-1 tat mRNA by dimer minizymes

Tomoko Kuwabara[1,2], Sergei V. Amontov[1], Masaki Warashina[1,2], Jun Ohkawa[1] and Kazunari Taira[1,2,*]

[1]National Institute of Bioscience and Human Technology, Agency of Industrial Science and Technology, MITI, Tsukuba Science City 305, Japan and [2]Institute of Applied Biochemistry, University of Tsukuba, Tennoudai 1-1-1, Tsukuba Science City 305, Japan

Received March 7, 1996; Revised and Accepted April 26, 1996

ABSTRACT

A minizyme is a hammerhead ribozyme with short oligonucleotide linkers instead of stem–loop II. In a previous study we demonstrated that a minizyme with high activity forms a dimeric structure with a common stem II. Because of their dimeric structure, minizymes are potentially capable of cleaving a substrate at two different sites simultaneously. In order to examine the properties of different kinds of minizyme, we constructed a number of minizymes with short oligonucleotide linkers (2–5 bases) instead of stem–loop II and examined their cleavage activities against HIV-1 tat mRNA. Analyses of melting curves, as well as Arrhenius plots, revealed that, in general, the longer the oligonucleotide linkers, the more stable and more active were the dimer minizymes. All minizymes examined cleaved the target substrate at two sites simultaneously. The activity of the dimer minizyme with a 5 nt linker was higher than that of the parental hammerhead ribozyme because the latter full-sized ribozyme was able to cleave at one site only.

INTRODUCTION

The hammerhead ribozyme is one of the smallest RNA enzymes (1–4). Because of its small size and potential utility as an antiviral agent, it has been extensively investigated in terms of the mechanism of its action and possible applications *in vivo* (2–8). It was first recognized as the sequence motif responsible for self-cleavage (*cis* action) in the satellite RNAs of certain viruses (9–11). The putative consensus sequence required for activity has three duplex stems and a conserved ‘core’ of two non-helical segments, plus an unpaired nucleotide at the cleavage site. The *trans*-acting hammerhead ribozyme, which was developed by Haseloff and Gerlach (3), consists of an antisense section (stems I and III) and a catalytic domain with a flanking stem–loop II section (Fig. 1a). In attempts to identify functional groups and to elucidate the role of the stem II region, various modifications and deletions have been made in this region (1,12–17). For the application of such enzymes as therapeutic agents for the treatment of infectious diseases, minimized hammerhead ribozymes (minizymes) seem to be particularly attractive (18). However, the activities of minizymes are two to three orders of magnitude lower than those of the parental hammerhead ribozymes, a result that led to the suggestion that minizymes might not be suitable as gene inactivating reagents (17). Thus, conventional hammerhead ribozymes with a deleted stem II (minizymes) have been considered to be crippled structures and have attracted minimal interest because of their extremely low activity, as compared to that of the full-sized ribozyme.

We reported recently the results of kinetic analyses that indicated that some minizymes have cleavage activity nearly equal to that of the wild-type hammerhead ribozyme and we presented evidence that minizymes with high level activity form dimeric structures (1). Such dimeric minizymes have two different binding sites and two catalytic cores (Fig. 1b). Therefore, it occurred to us that it might be possible to construct dimeric minizymes that would cleave a target substrate at two sites simultaneously, with a resultant overall increase in the efficiency of degradation of the target RNA. These dimeric minizymes could be designed in such a way that they would only be able to form binding sites complementary to the substrate sequence as a result of the formation of heterodimers (Fig. 1c). The stability of the dimeric structure depends on Mg^{2+} ions and the number of G-C pairs in stem II of the dimeric minizyme (1). In order to define the number of G-C pairs required for activity in such a system, we designed dimeric minizymes with two to five G-C pairs in the stem II region (Fig. 2).

We selected HIV-1 tat mRNA as the target substrate of our dimeric minizymes (Fig. 3; 19). Hammerhead ribozymes can cleave any RNA with a high degree of sequence specificity via recognition of the Watson–Crick type at stems I and III. The target site must contain the NUX triplet (N = G, A, C or U, X = A, C or U), but the efficiency of cleavage depends on the combination of N and X (20–25). In this study, dimeric minizymes were designed to cleave HIV-1 tat mRNA at two GUC triplets (GUC triplet-1 and GUC triplet-2, located 51 and 189 nt, respectively, from the 5′-end

* To whom correspondence should be addressed at: Institute of Applied Biochemistry, University of Tsukuba, Tennoudai 1-1-1, Tsukuba Science City 305, Japan

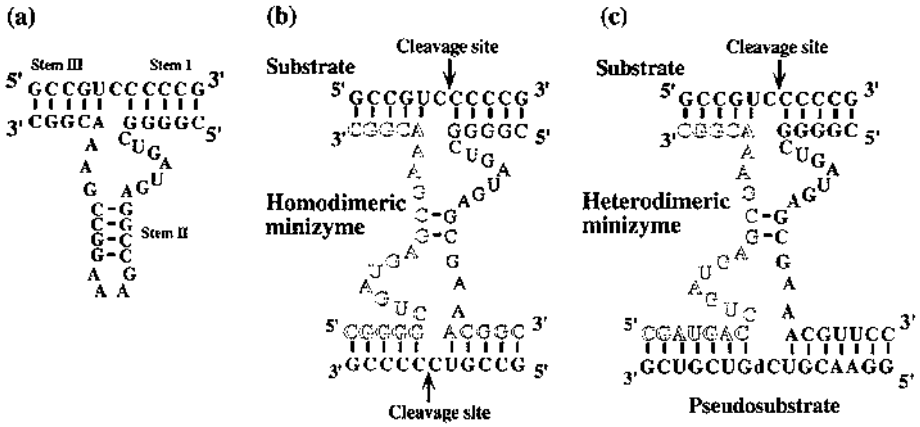

Figure 1. Secondary structures of the previously analyzed (**a**) hammerhead ribozyme (R32) and its substrate (R11), (**b**) the homodimeric 2 bp minizyme (Mz22-GC) and (**c**) the heterodimeric 2 bp minizyme (MzL–MzR heterodimer). The heterodimeric minizyme, shown in (c), can generate two different binding sites: one is complementary to the sequence of R11 (top) and the other is complementary to an uncleavable pseudosubstrate. The presence of the pseudosubstrate can enhance cleavege of the substrate (1).

of the substrate; Fig. 3) with an internucleotide distance of 138 nt between them. A computer-generated (MulFold) prediction of the secondary structure of HIV-1 tat mRNA is shown in Figure 3.

In this report we describe the physical properties of each heterodimeric minizyme and we demonstrate that all heterodimeric minizymes tested were capable of cleaving the HIV-1 tat mRNA at both GUC triplets simultaneously. Moreover, we show that the activity of the minizymes increased with increases in the length of the linker sequence of the dimer.

MATERIALS AND METHODS

Synthesis of ribozymes

Ribozymes and their corresponding short substrates were chemically synthesized on a DNA/RNA synthesizer (model 394; Applied Biosystems, Foster City, CA) and purified by polyacrylamide gel electrophoresis as described previously (26–28). Reagents for RNA synthesis were purchased from Perkin Elmer, Applied Biosystems Division (ABI, Foster City, CA). The oligonucleotides were purified as described in the user bulletin from ABI (no. 53, 1989) with minor modifications.

Preparation of HIV-1 tat mRNA, the target substrate, by transcription

The template for the HIV-1 tat mRNA substrate was prepared by PCR from a template plasmid, pcD-SRα/tat (29). The primer for the sense strand contained a T7 promoter. Transcription and gel electrophoretic purification of the HIV-1 tat mRNA substrate were performed as described elsewhere (30).

Kinetic measurements

Reaction rates were measured, in 25 mM $MgCl_2$ and 50 mM Tris–HCl, pH 8.0 (adjusted at each temperature), under ribozyme saturating (single turnover) conditions either at 37°C [measurements of k_{cat}, k_{obs} and $K_{d(app)}$] or at various temperatures from 20 to 60°C [for measurements of the dependence on temperature (Arrhenius plots)]. The reactions were usually initiated by the addition of $MgCl_2$ to a buffered solution that contained the minizymes and the substrate and mixtures were then incubated at the chosen temperature. The 5′-terminus of the short substrate (S19), which included GUC triplet-2 and has the sequence 5′-CAGAACA-(GUC)-AGACUCAUC-3′ (the binding sites for the dimeric minizymes, 18 nt in all, are underlined and the GUC triplet is shown in parentheses), was labeled with [γ-^{32}P]ATP by T4 polynucleotide kinase (Takara Shuzo). The HIV-1 tat mRNA was labeled internally with [α-^{32}P]CTP during transcription *in vitro* by T7 RNA polymerase (Takara Shuzo). In all cases, kinetic measurements were made under conditions where all the available substrate was expected to form a Michaelis–Menten complex, at high concentrations of minizymes (from 50 nM to 10 μM).

Reactions were stopped by removal of aliquots from the reaction mixture at appropriate intervals and mixing them with an equivalent volume of a solution that contained 100 mM EDTA, 9 M urea, 0.1% xylene cyanol and 0.1% bromophenol blue. The substrate and the products of the reaction were separated by electrophoresis on a 5–20% polyacrylamide–7 M urea denaturing gel and were detected by autoradiography. The extent of cleavage was determined by quantitation of radioactivity in the bands of substrate and products with a Bio-Image Analyzer (BAS2000; Fuji Film, Tokyo).

Measurements of melting temperatures (T_m) of the dimeric minizymes

In order to determine the T_m of the duplex regions (G-C pairs) with 2, 3, 4 and 5 bp, respectively, in stem II of the dimeric minizymes, we monitored the thermal denaturation of the ribozymes with a UV spectrophotometer (model 2100S; Shimadzu, Kyoto). Solutions of the dimeric minizymes (2 μM) were prepared in 50 mM Tris–HCl buffer, pH 8.0, containing 25 mM $MgCl_2$. After degassing, these samples, without Mg^{2+} ions, were preheated at 80°C for 3 min and then slowly cooled to 5°C over the course of 20 min and then a concentrated solution of Mg^{2+} ions was added to each sample to give a final concentration of $MgCl_2$ of 25 mM. The absorption of the samples at 260 nm was monitored continuously at 5°C for 10 min and then the temperature was raised from 5 to 80°C at a rate of 1°C/min. The T_m was determined by plotting the derivative of the thermal denaturation curve (Fig. 6).

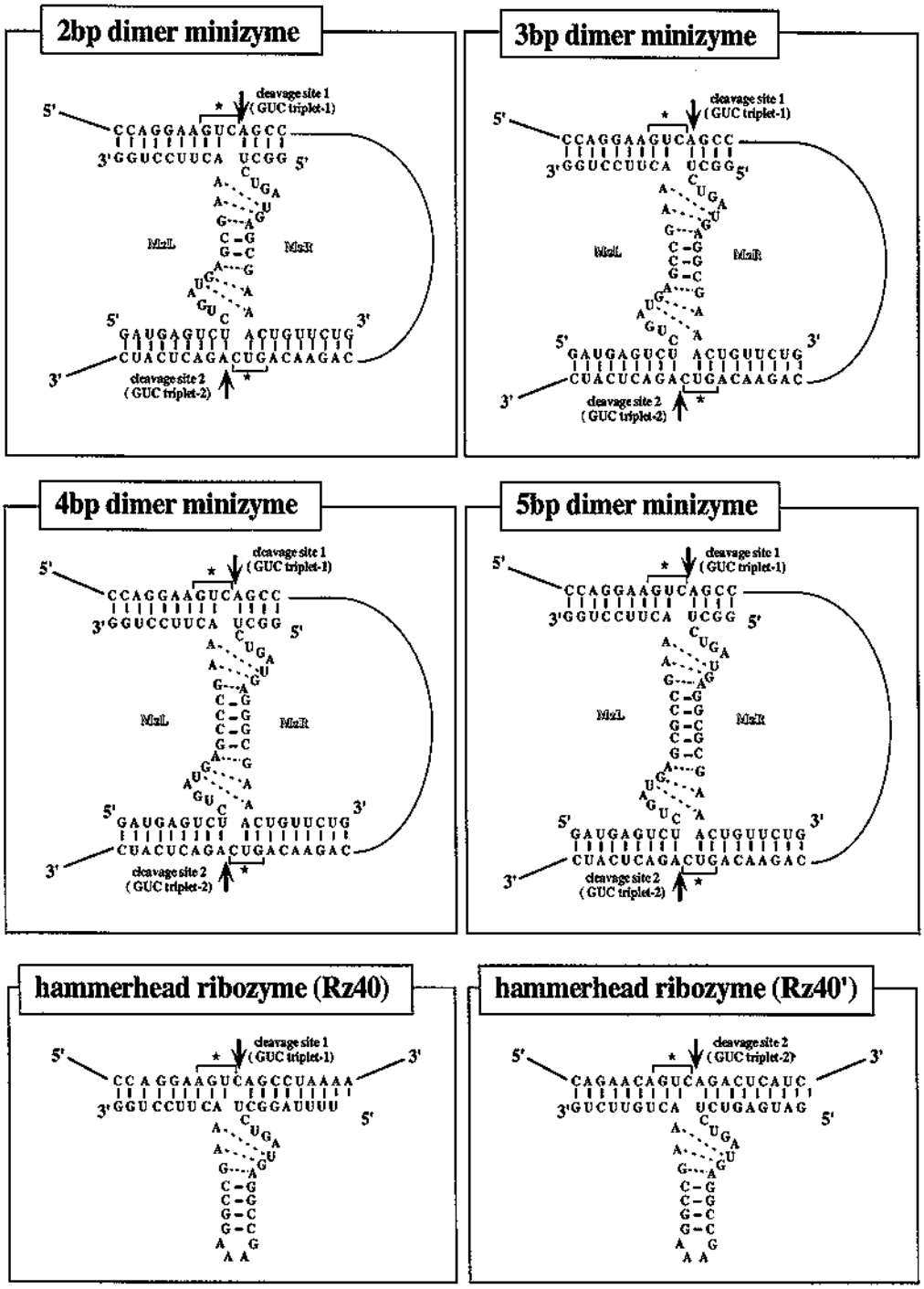

Figure 2. The secondary structures of the various dimeric minizymes used in this study. As controls we used the parental hammerhead ribozyme (Rz40), targeted to GUC triplet-1, and Rz40′, targeted to a 19mer substrate (S19) that contained GUC triplet-2 (see Fig. 3).

RESULTS AND DISCUSSION

Simultaneous cleavage of HIV-1 tat mRNA at two independent sites by dimeric minizymes

We demonstrated previously that minizymes with high level activity form dimeric structures (1). The stability of dimeric minizymes depends on the concentration of Mg^{2+} ions, whether or not the minizymes are bound to their substrate and the number of G-C pairs in the common stem II region. Since the dimeric minizymes were expected to cleave substrates at two independent sites, we examined several kinds of dimeric minizyme, which differed from one another in the length of stem II, for their ability to serve as gene inactivating agents. The dimeric minizymes used in this study are shown in Figure 2. We use the term 2 bp dimeric minizyme to describe the dimeric minizyme with two G-C pairs.

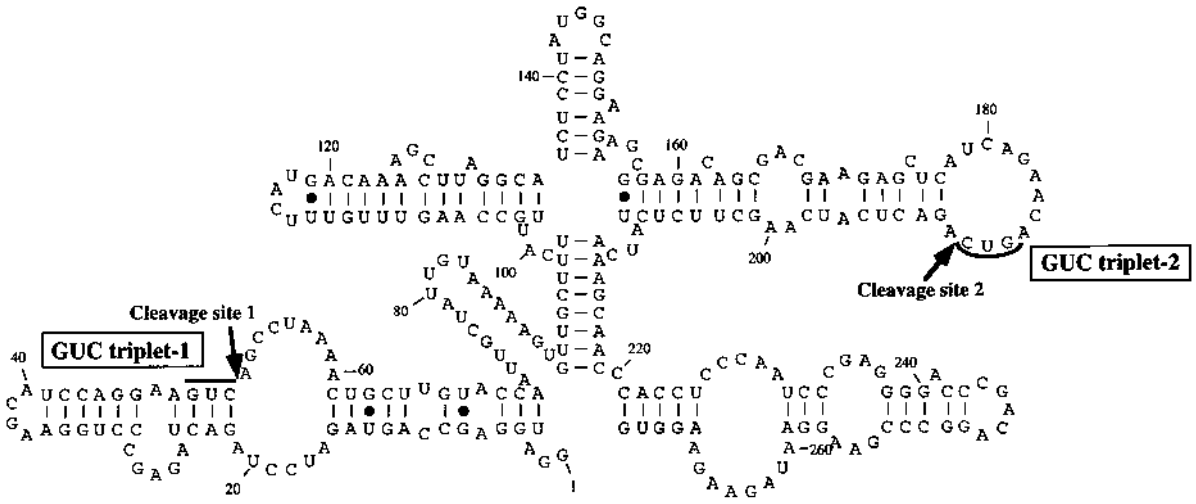

Figure 3. The secondary structure of HIV-1 tat mRNA, as predicted by a computer program. Cleavage sites 1 (GUC triplet-1) and 2 (GUC triplet-2) are indicated by arrows.

Thus, the 3 bp, 4 bp and 5 bp dimeric minizymes have three, four and five G-C pairs, respectively, in the stem II region. The substrate selected in this study was HIV-1 tat mRNA, which is 272 nt in length and whose predicted secondary structure is shown in Figure 3. Two target sites were selected in this substrate (Figs 3 and 4a). Cleavage at GUC triplet-1 in HIV-1 tat mRNA generates fragments of 51 (fragment A in Fig. 4a) and 221 nt (fragment B) in length. Similarly, cleavage at GUC triplet-2 generates fragments of 189 (C) and 83 nt (D) in length. Thus, complete cleavage at both GUC triplets should generate an additional fragment (E) of 138 nt in length. As a control, we also examined a parental wild-type ribozyme (Rz40, Fig. 2) targeted to GUC triplet-1.

The expected products of the various cleavages are displayed in the autoradiogram in Figure 4b. All the dimeric minizymes tested cleaved the long HIV tat mRNA substrate at two independent sites simultaneously. The strength of the activity depended on the number of G-C pairs in the stem II region: the activity increased with increasing numbers of G-C pairs. As can be seen from Figure 4b, significant cleavage activity was observed with the 4 bp and 5 bp dimeric minizymes. For simultaneous cleavage at two sites in the substrate by the dimeric minizymes, it seems that it was important that the two catalytic cores were stabilized by a strong dimeric structure. Such a hypothesis explains why the 5 bp dimeric minizyme had the highest activity.

Our previous kinetic analysis demonstrated that when a short substrate (11mer) was used, a dimeric minizyme with two G-C base pairs retained 65% of the activity of the parental hammerhead ribozyme (1). However, our present results demonstrate that when the target site is embedded in a long RNA substrate, a very stable common stem II is required (depending on the sequence of the target site; see below). Accordingly, as judged from the rate of disappearance of the substrate (Fig. 4b), the cleavage activity of the 5 bp dimeric minizyme was even higher than that of the full-sized hammerhead ribozyme, because the latter full-sized ribozyme was able to cleave at the GUC triplet-1 only.

Our present examination of dimeric minizymes demonstrates that in attempts to design gene inactivating agents, we should also consider dimeric minizymes that can simultaneously cleave a substrate at two independent sites.

Kinetic parameters for the cleavage of a short 19mer substrate by dimeric minizymes

In order to characterize in further detail the properties of dimeric minizymes, we determined the kinetic parameters of cleavage (Fig. 5) using a short 19mer substrate (S19) that contained GUC triplet-2. The sequence of this substrate is shown in Figure 2. We chose a substrate that contained GUC triplet-2 and not GUC triplet-1 because, from our computer prediction, we expected the former sequence to be less likely to form inactive dimeric minizymes. In order to ensure that we measured only the rate of the pure chemical cleavage step (k_{cleav}), all reactions in this study were carried out under single turnover conditions.

Table 1. The activities of various ribozymes[a]

Ribozyme	$k_{cat}^{(min-1)}$	$K_d^{(app)}$ (μM)
Dimeric minizymes		
2 bp dimer minizyme	0.006	1.0
3 bp dimer minizyme	0.014	0.55
4 bp dimer minizyme	0.042	0.067
5 bp dimer minizyme	0.24	0.22
Reported homodimeric minizymes[b]		
Mz22–GC	2.5	5.1
Mz24–GCGC	2.2	0.17
Reported heterodimeric minizymes[b]		
Mz24–UGAC/GTTC	0.12	
Mz24–UGAC/GUAA	0.032	
Mz21–C/Mz21–G	0.015	15

[a]All reaction rates were measured, in 25 mM $MgCl_2$ and 50 mM Tris–HCl, pH 8.0, under ribozyme saturating (single turnover) conditions at 37°C. In all cases kinetic measurements were made under conditions where all the available substrate was expected to form a Michaelis–Menten complex, with high concentrations of ribozyme (from 50 nM to 10 μM).
[b]Taken from Amontov and Taira (1).

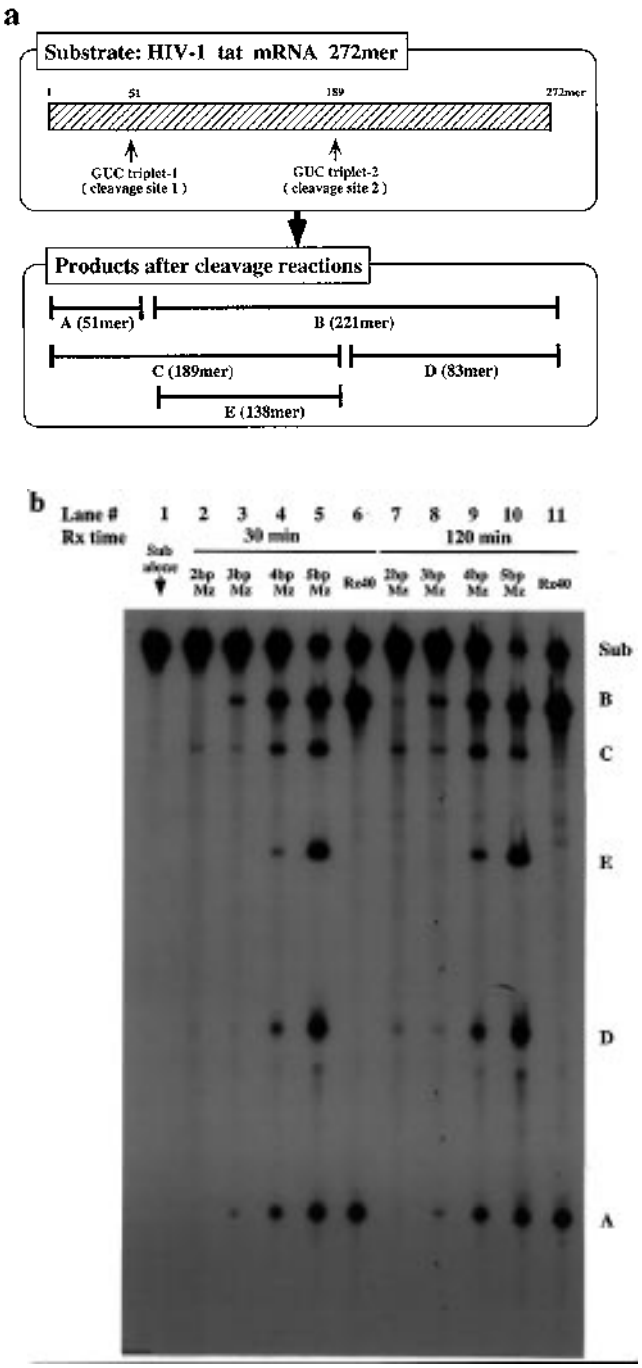

Figure 4. Cleavage activities of dimeric minizymes with stem II regions of different lengths and the full-sized hammerhead ribozyme (Rz40). (**a**) Schematic illustration of cleavage products. Cleavage at GUC triplet-1 in HIV-1 tat mRNA (Sub) generates fragments of 51 (fragment A) and 221 nt (fragment B) in length. Similarly, cleavage at GUC triplet-2 generates fragments of 189 (C) and 83 nt (D) in length. Complete cleavage at both GUC triplets generates an additional fragment (E) of 138 nt in length. (**b**) Autoradiogram of the various cleavage reactions. Bands in each lane represent the reaction products formed after 30 (lanes 2–6) and 120 min (lanes 7–11) at 37°C in 50 mM Tris–HCl, pH 8.0, and 25 mM $MgCl_2$. Concentrations: internally [α-^{32}P]-labeled substrate (Sub, HIV-1 tat mRNA), 100 nM; ribozyme (MzL and MzR of each heterodimeric minizyme and Rz40), 1 µM. Lane 1, control (no ribozyme); lanes 2 and 7, 2 bp dimeric minizyme; lanes 3 and 8, 3 bp dimeric minizyme; lanes 4 and 9, 4 bp dimeric minizyme; lanes 5 and 10, 5 bp dimeric minizyme; lanes 6 and 11, Rz40.

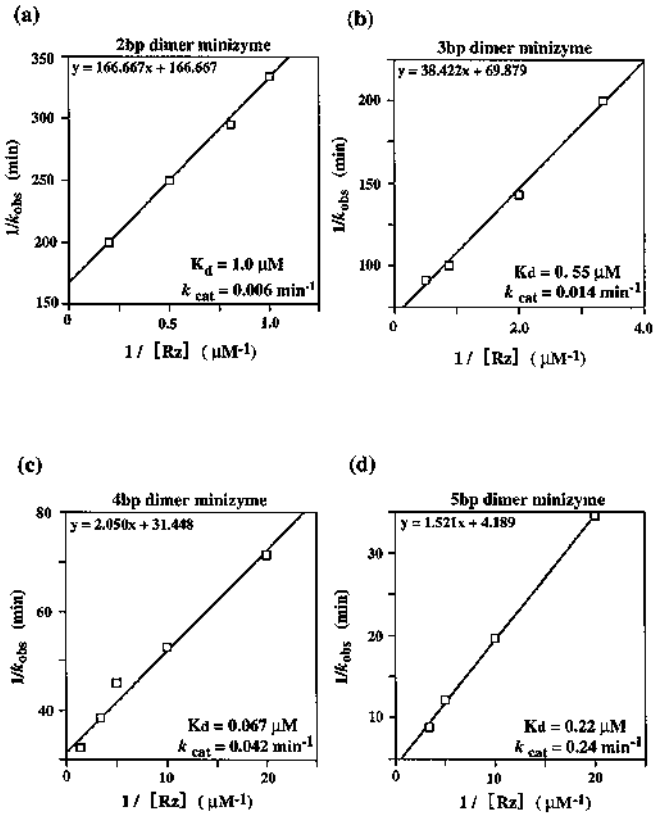

Figure 5. Lineweaver–Burk plots of data obtained under single turnover conditions for each dimeric minizyme. Calculated values of k_{cat} and $K_{d(app)}$ are shown in each panel and they are also tabulated in Table 1.

The rate constants of the dimeric minizymes determined with the short S19 substrate are shown in Table 1. As can be seen from Table 1, the 5 bp dimeric minizyme had the highest cleavage activity, with a k_{cat} of 0.24/min, which was 40 times greater than that of the 2 bp dimeric minizyme. The cleavage activity of dimeric minizymes increased with increases in the number of G-C pairs in the stem II region of the dimeric minizyme, in agreement with the observations made with the much longer HIV-1 tat mRNA. Thus, it is clear that even for a short substrate, a stable common stem II is preferable. The rate constants of these dimeric minizymes were lower than those of homodimeric minizymes, the structure of one of which is shown in Figure 1b, but the heterodimeric minizymes in this study had higher activities than those of previously studied heterodimers (1). In a previous study, we investigated the rate constant of a heterodimeric minizyme using a cleavable substrate in the presence of an uncleavable pseudosubstrate (Fig. 1c) and the presence of the pseudosubstrate was shown to enhance cleavage of the substrate (1). Similarly, the present heterodimers would be expected to exhibit higher activity in the presence of a second substrate that contained the GUC triplet-1.

We demonstrated previously that $K_{d(app)}$ characterizes the dimerization process (1). In order to investigate the stability of the dimeric minizymes used in this study, we determined $K_{d(app)}$ for each under single turnover conditions from Lineweaver–Burk plots (Fig. 5). The $K_{d(app)}$ of the dimeric minizymes decreased

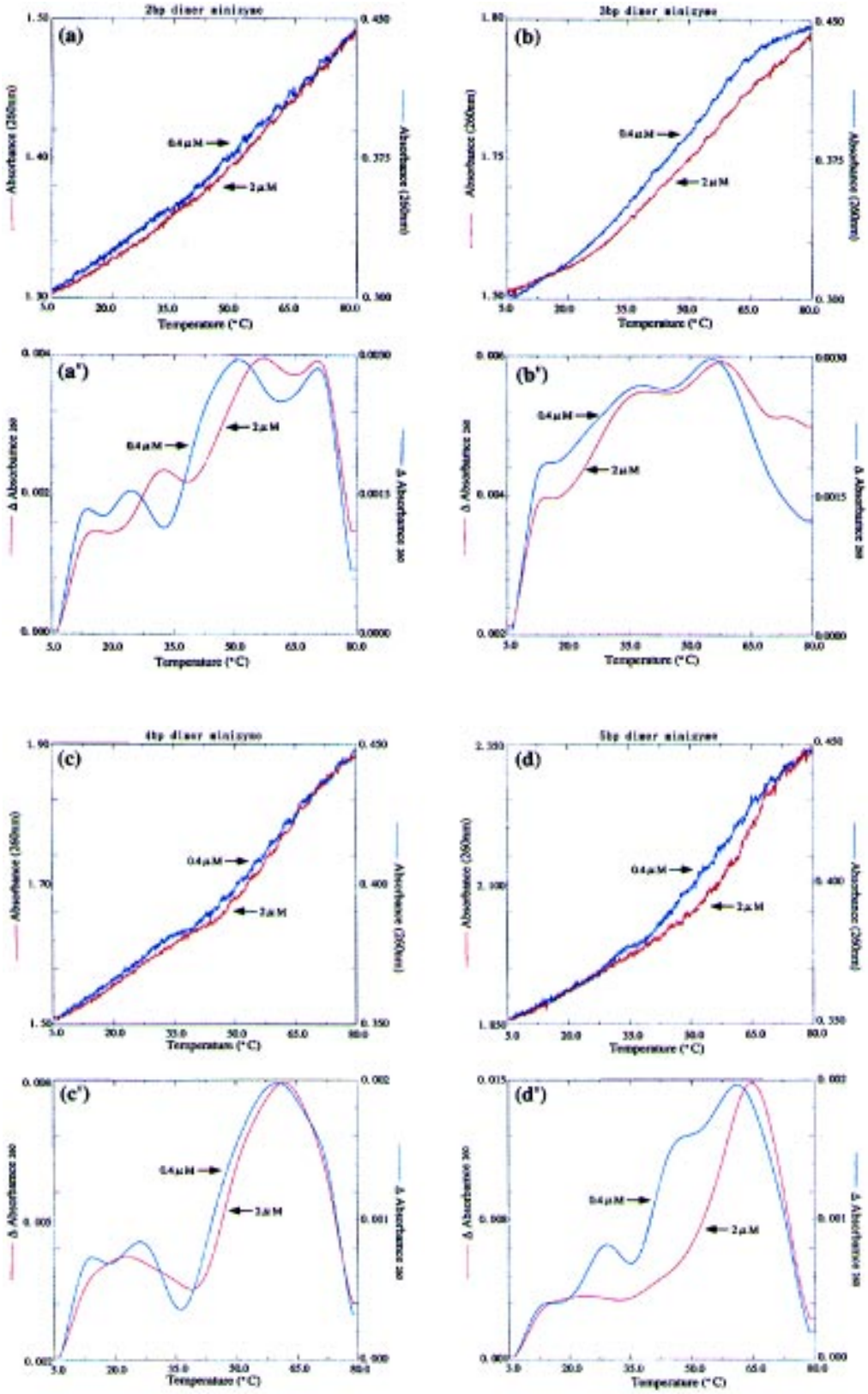

Figure 6. Melting curves (**a**–**d**) and derivative curves (**a′**–**d′**) for the dimeric minizymes. Buffer conditions 50 mM Tris–HCl, pH 8.0, containing 25 mM $MgCl_2$. Red lines, 2 μM dimeric minizyme; blue lines, 0.4 μM dimeric minizyme.

with increasing numbers of G-C pairs in the stem II region of the dimeric minizyme. The previously determined $K_{d(app)}$ of the homodimeric minizyme with two G-C pairs was 5.1 μM and that of a homodimeric minizyme with four G-C pairs was 0.17 μM (1). As compared with these values, in general, the values of $K_{d(app)}$ of the present dimeric minizymes (heterodimeric minizymes) tended to be lower. In accordance with the previous observation, in general, the longer the common stem II, the lower the $K_{d(app)}$ value. However, for some unknown reason, the $K_{d(app)}$ of the 4 bp dimeric minizyme was unexpectedly low. The value of $K_{d(app)}$ for the 4 bp dimeric minizyme does not reflect the melting temperature for dissociation of the dimeric structure, as described in the next section.

Melting curves for dimeric minizymes determined in the absence of substrates

In order to examine the effects of the G-C pairs in the stem II region on the stability of the dimeric minizymes, we investigated the melting properties of each dimeric minizyme in the absence of substrates (Fig. 6). The reaction conditions for the generation of melting curves were the same as those in the kinetic experiments. In particular, the reaction mixtures included 25 mM $MgCl_2$. The concentrations of minizymes were 2 μM [higher than the respective values of $K_{d(app)}$]. Moreover, in order to distinguish intermolecular melting from intramolecular melting, the dependence of T_m on the concentration of each minizyme was examined. Thus, thermal denaturation profiles were also recorded at the 5-fold lower concentration of minizymes of 0.4 μM.

Figure 6 shows the thermal denaturation profiles of the dimeric minizymes. As can be seen from derivative curves for the various dimeric minizymes (Fig. 6a′–d′), many transitions were observed, an indication that more interactions were occurring than had been predicted from the structure shown in Figure 2. In order to identify the T_m that corresponds to melting of the stem II region of the dimeric minizymes, we tried to examine the concentration dependence of T_m. For the 2 bp dimeric minizyme (Fig. 6a′), the T_m of the stem II region was identified as 55.0°C at 2 μM minizyme and it shifted to 51.0°C when a 5-fold lower concentration (0.4 μM) of minizyme was used. While we also detected other T_m, for example, at >65°C, such melting was not concentration dependent, an indication that it reflected intramolecular interactions.

Similarly, we identified the T_m of the G-C pairs in the 3 bp dimeric minizyme as 57.5°C (Fig. 6b′) and it shifted to 55.0°C upon dilution. In this case, other melting temperatures were concentration independent. For the 4 bp dimeric minizyme (Fig. 6c′), the T_m of G-C pairs was 62.0°C at 2 μM and shifted to 59.8°C at a 5-fold lower concentration. The T_m for the 5 bp dimeric minizyme was determined to be 64.8°C. At the lower concentration, it shifted to 61.3°C. These data demonstrate that the T_m of dimeric minizymes, which reflects the stability of the dimeric structure, increased with increases in the length of the stem II region: when the concentration of the minizymes was 2 μM, the T_m of the stem II regions of 2 bp, 3 bp, 4 bp and 5 bp dimers were, respectively, 55.0, 57.5, 62.5 and 64.8°C.

The existence of other, lower, concentration-dependent melting temperatures at ~20°C indicated that other intermolecular interactions also existed. Such interactions might include those between the 5′-part and the 3′-part of the substrate binding sites.

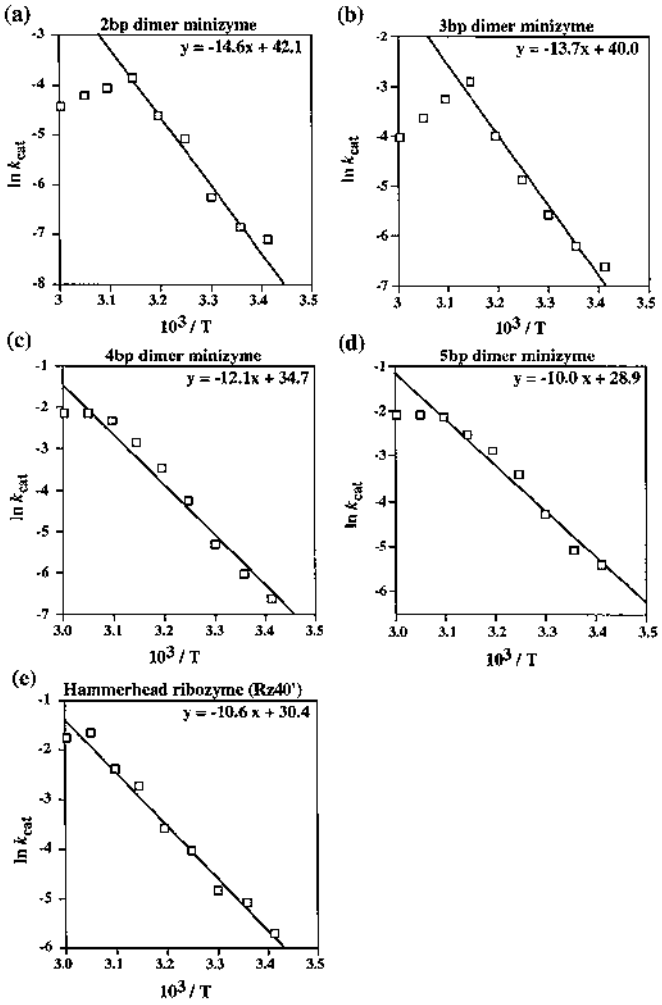

Figure 7. Arrhenius plots of data obtained from reactions with dimeric minizymes and Rz40′ under single turnover conditions. Reactions were carried out in 50 mM Tris–HCl, pH 8.0, 25 mM $MgCl_2$. Concentrations: 5′-^{32}P-labeled substrate (S19), 50 nM; 2 bp dimeric minizyme, 5 μM; 3 bp dimeric minizyme, 3 μM; 4 and 5 bp dimeric minizyme, 2 μM; Rz40′, 300 nM.

Arrhenius plots

Since the melting temperatures reported in the previous section represented the dissociation of dimers in the absence of any substrate, we next examined the thermal stability of each dimeric minizyme in the active complex with its substrate by examining the dependence of the cleavage activity on temperature. The substrate used in this analysis was same as that used for kinetic measurements (S19).

The activation energy for a reaction can be determined by measuring the rate constant of the reaction (k) at different temperatures and plotting ln$k$ versus 1/T (to yield a so-called Arrhenius plot, e.g. Fig. 7). The Arrhenius plot itself may be non-linear if different steps become the rate determining step at different temperatures (31). In some cases, the plot may show a sharp change in slope at the temperature (transition temperature) at which the rate determining step changes from one to another. Arrhenius plots have been used to detect such changes in standard enzyme-catalyzed reactions and also in ribozyme-catalyzed reactions (3,31).

Table 2. Thermodynamic parameters

Ribozyme	Ea (kcal/mol)	$\Delta G^{\neq}$ (kcal/mol) at 35°C	$\Delta H^{\neq}$ (kcal/mol) at 35°C	$\Delta s^{\neq}$ (eu) at 35°C
2 bp dimer minizyme	29.0	21.2	28.4	23.4
3 bp dimer minizyme	27.2	21.0	26.6	18.2
4 bp dimer minizyme	24.0	20.7	23.4	8.8
5 bp dimer minizyme	20.0	20.1	19.4	–2.3
Hammerhead ribozyme (Rz40′)	21.1	20.5	20.5	–0.2

The results of our analysis, namely the Arrhenius plots, are shown in Figure 7. Arrhenius activation energies were calculated from the linear regions of the graphs to be 29.0 kcal/mol (from 20 to 45°C) for the 2 bp dimeric minizyme, 27.2 kcal/mol (from 20 to 45°C) for the 3 bp dimeric minizyme, 24.0 kcal/mol (from 20 to 50°C) for the 4 bp dimeric minizyme and 20.0 kcal/mol (from 20 to 50°C) for the 5 bp dimeric minizyme. While the Arrhenius activation energy of the full-sized hammerhead ribozyme, Rz40′ (Fig. 2), was 21.1 kcal/mol, the corresponding Arrhenius energy of the 2 bp dimeric minizyme turned out to be the highest among those of all the minizymes examined in this study (Table 2).

Arrhenius parameters were converted to thermodynamic activation parameters by application of the transition state theory. The free energy of activation, $\Delta G^{\neq}$, is directly related to the rate of the reaction. $\Delta G^{\neq}$ is given by $-RT\ln(kh/k_BT)$, where k is the rate constant at temperature T, h is Planck's constant and k_B is Boltzmann's constant. The enthalpy of activation, $\Delta H^{\neq}$, is a measure of the energy barrier that must be overcome by the reacting molecules. $\Delta H^{\neq}$ is given by $E_a - RT$, where R is the gas constant and E_a is the energy of activation. The entropy of activation, $\Delta S^{\neq}$, is a measure of the fraction of reactants that have sufficient activation enthalpy and can actually react; $\Delta S^{\neq}$ includes, for example, concentration and solvent effects, steric requirements and orientational requirements. $\Delta S^{\neq}$ is equivalent to $(\Delta H^{\neq} - \Delta G^{\neq})/T$.

The calculated energy parameters for the minizyme-catalyzed single turnover reactions at 35°C are listed in Table 2. Naturally, $\Delta G^{\neq}$ (k_{cat}) is a function of $\Delta H^{\neq}$ and $T\Delta S^{\neq}$. It is of interest that, while $\Delta S^{\neq}$ is negative for the previously examined ribozyme (31) and also for the relatively active ribozymes, such as Rz40′ and the 5 bp dimeric minizyme examined in this study (Table 2), indicating a more precise conformation in the transition state than in the Michaelis–Menten complex, $\Delta S^{\neq}$ is positive for the less active dimeric minizymes, such as the 2 bp, 3 bp and 4 bp minizymes (Table 2). This result indicates that the activated Michaelis–Menten complexes of the less active dimeric minizymes require more precise orientation than their respective transition state structures. It is also to be noted that, while the value of $\Delta S^{\neq}$ differs dramatically among the minizymes, the discrepancy is compensated for by $\Delta H^{\neq}$, such that $\Delta G^{\neq}$ remains almost the same for all the ribozymes examined in this study.

In the case of the dimeric minizymes with a short common stem II, as can be seen in Figure 7, the rate of the reaction decreased at high temperatures (above 45–50°C). This decrease occurred because the formation of active dimeric structures at such high temperatures was hampered by thermal melting. (Therefore, the rates of reactions above 45–50°C do not reflect k_{cat}.) This conclusion is in agreement with our deduction from the derivative curves of T_m (Fig. 6) that the disruption of dimeric structures, which depended on the stability of G-C pairs in the stem II region, began when the temperature was raised above 40°C. Therefore, in general, the shorter the common stem II, the lower the transition temperature for the loss of activity (Fig. 7).

Conclusion

In this study we examined a new form of shortened hammerhead ribozymes, namely dimeric minizymes, in terms of their activities as gene inactivating agents. Although our previously studied homodimeric minizyme, with two G-C pairs in the common stem II (Fig. 1b), retained 65% of the activity of the parental hammerhead ribozyme (Fig. 1a), the present analysis demonstrated that the longer the common stem II, the higher the cleavage activity of the dimeric minizyme, at least when the target site is part of HIV-1 tat mRNA. The activity was correlated with the stability of the dimeric minizymes, as determined from thermal melting curves, as well as from Arrhenius plots. Since these dimeric ribozymes successfully cleaved the long target RNA at two independent sites, it appears that the dimeric minizyme is a new variant of the conventional hammerhead ribozyme that has considerable potential utility as a gene inactivating agent (8,32–36).

REFERENCES

1 Amontov,S.V. and Taira,K. (1996) *J. Am. Chem. Soc.*, **118**, 1624–1628.
2 Symon,R,H. (1989) *Trend Biochem. Sci.*, **14**, 445–450.
3 Uhlenbeck,O.C. (1987) *Nature*, **328**, 596–600.
4 Haseloff,J. and Gerlach,W.L. (1988) *Nature*, **334**, 585–591.
5 Fedor,M.J. and Uhlenbeck,O.C. (1992) *Biochemistry*, **31**, 12042–12054.
6 Dahm,S.C., DerrickW.B. and Uhlenbeck,O.C. (1993) *Biochemistry*, **32**, 13040–13045.
7 Hertel,K.J., Herschlag,D. and Uhlenbeck,O.C. (1994) *Biochemistry*, **33**, 3374–3385.
8 Sarver,M., Cantin,E., Chang,P., Ladne,P., Stephens,D., Zaia,J. and Rossi,J. (1990) *Science*, **247**, 1222–1225.
9 Proby,G.A., Bakos,J.T., Buzayan,J.M. and Bruening,G. (1986) *Science*, **231**, 1577–1580.
10 Hutchins,C.J., Rathjen,P.D., Foster,A.C. and Symons,R.H. (1986) *Nucleic Acids Res.*, **14**, 3627–3640.
11 Buzayan,J.M., Gerlach,W.L. and Bruening,G. (1986) *Nature*, **323**, 349–353.
12 Goodchild,J. and Kohli,V. (1991) *Arch. Biochem. Biophys.*, **284**, 386–391.
13 McCall,M.J., Hendry,P. and Jennings,P.A. (1992) *Proc. Natl. Acad. Sci. USA*, **89**, 5710–5714.
14 Tuschl,T. and Eckstein,F. (1993) *Proc. Natl. Acad. Sci. USA*, **90**, 6991–6994.
15 Thomson,J.B., Thschl,T. and Eckstein,F. (1993) *Nucleic Acids Res.*, **21**, 5600–5603.
16 Fu,D., Benseler,F. and McLaughlin,L.W. (1994) *J. Am. Chem. Soc.*, **116**, 4591–4598.
17 Long,D.M. and Uhlenbeck,O.C. (1994) *Proc. Natl. Acad. Sci. USA*, **91**, 6977–6981.
18 Hendry,P., McCall,M.J., Santiago,F.S. and Jennings,P.A. (1995) *Nucleic Acids Res.*, **23**, 3922–3927.
19 Ohkawa,J., Yuyama,N., Takebe,Y., Nishikawa,S. and Taira,K. (1993) *Proc. Natl. Acad. Sci. USA*, **90**, 11302–11306.
20 Koizumi,M., Iwai,S. and Ohtsuka,E. (1988) *FEBS Lett.*, **228**, 228–230.

21 Ruffer,D.E., Stormo,G.D. and Uhlenbeck,O.C. (1990) *Biochemistry*, **29**, 10696–10702.
22 Sheldon,C.C. and Symons,R.H. (1989) *Nucleic Acids Res.*, **17**, 5679–5685.
23 Perriman,R., Delves,A. and Gerlach,W.L. (1992) *Gene*, **113**, 157–163.
24 Shimayama,T., Nishikawa,S. and Taira,K. (1995) *Biochemistry*, **34**, 3649–3654.
25 Zoumadakis,M. and Tabler,M. (1995) *Nucleic Acids Res.*, **23**, 1192–1196.
26 Shimayama,T., Nishikawa,F., Nishikawa,S. and Taira,K. (1993) *Nucleic Acids Res.*, **21**, 2605–2611.
27 Sawata,S., Shimayama,T., Komiyama,M., Kumar,P.K.R., Nishikawa,S. and Taira,K. (1993) *Nucleic Acids Res.*, **21**, 5656–5660.
28 Shimayama,T. (1994) *Gene*, **149**, 41–46.
29 Takebe,Y., Seiki,M., Fujisawa,J., Pamala,H., Yokota,K., Arai,K., Yoshida,M. and Arai,N. (1988) *Mol. Cell. Biol.*, **8**, 466–472.
30 Taira,K., Nakagawa,K., Nishikawa,S. and Fukukawa,K. (1991) *Nucleic Acids Res.*, **19**, 5152–5130.
31 Takagi,Y. and Taira,K. (1995) *FEBS Lett.*, **361**, 237–276.
32 Homann,M., Tzortzakaki,M., Rittner,K., Sczakiel,S. and Tabler,M. (1993) *Nucleic Acids Res.*, **21**, 2809–2814.
33 Altman,S. (1993) *Proc. Natl. Acad. Sci. USA*, **90**, 10898–10900.
34 Marschall,P., Thompson,J.B. and Eckstein,F. (1994) *Cell. Mol. Neurobiol.*, **14**, 523–538.
35 Murray,J.A.H. (ed.) (1992) *Antisense RNA and DNA*. Wiley-Liss, New York, NY.
36 Erickson,R.P. and Izant,J.G. (eds) (1992) *Gene Regulation: Biology of Antisense RNA and DNA*. Raven Press, New York, NY.